International Journal of Pharmaceutics 663 (2024) 124594

Contents lists available at ScienceDirect

International Journal of Pharmaceutics

journal homepage: www.elsevier.com/locate/ijpharm

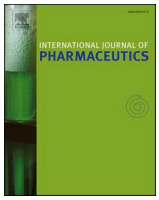

Sustained release of 3D printed bupropion hydrochloride tablets bearing Braille imprints for the visually impaired

Chrystalla Protopapa [a], Angeliki Siamidi [a], Laura Andrade Junqueira [d], Siva Kolipaka [b], Atabak Ghanizadeh Tabriz [c], Dennis Douroumis [b,d,*], Marilena Vlachou [a,**]

[a] Section of Pharmaceutical Technology, Department of Pharmacy, National and Kapodistrian University of Athens, 157 84 Athens, Greece
[b] Centre for Research Innovation, University of Greenwich, Medway Campus, Chatham Maritime, Chatham ME4 4TB, UK
[c] School of Life Sciences, University of Nottingham, NG7 2RD, UK
[d] Delta Pharmaceutics Ltd., 1- 3 Manor Road, Chatham, ME4 6AE Kent, UK

ARTICLE INFO

Keywords:
Bupropion hydrochloride
3D printing
Liquid crystal display (LCD)
Braille imprint
Personalized medicine
Sustained release

ABSTRACT

3D printing has been introduced as a novel approach for the design of personalized dosage forms and support patient groups with special needs that require additional assistance for enhanced medication adherence. In this study liquid crystal display (LCD) is introduced for the development of sustained release bupropion·HCl printed tablets. The optimization of printing hydrogel inks was combined with the display of Braille patterns on the tablet surface for blind or visually impaired patients. Due to the high printing accuracy, the Braille patterns could be verified by blind patients and provide the required information. Further characterization revealed the presence of BUP in amorphous state within the photopolymerized resins. The selection of poly(ethylene glycol) (PEG)-diacrylate (PEGDA) of different molecular weights and the presence of surfactants or solubilizers disrupted the resin photopolymerization, thus controlling the BUP dissolution rates. A small batch scale-up study demonstrated the capacity of LCD to print rapidly a notable number of tablets within 24 min.

1. Introduction

Personalized medicine has been proposed as a remedy to ensure the safe, efficient utilization and minimization of the side effects of medications with narrow therapeutic indices, like bupropion (BUP), which necessitate precise dosing to preserve treatment efficacy and patients' safety (Mini and Nobili, 2009; Trenfield et al., 2018). As BUP is typically administered in single discrete strengths, it has become customary for patients, caregivers, or medical staff to split tablets or prepare formulations on the spot (e.g., by crushing the tablets) to reach the desired dose. Nevertheless, these practices present the risk of inaccurate dosing, variations in dosage, and dose dumping, all of which could lead to significant therapeutic repercussions (Brian and Antoine Al-Achi, 2015; Hill et al., 2009). Another reason why contemporary society is increasingly inclined towards personalized therapy is that the dosage needs to vary significantly among individuals due to variations in physical attributes, such as body weight, surface area, age, and also pharmacokinetic factors (including metabolic capacity, drug clearance, and organ function) (Breitkreutz and Boos, 2007). In particular, safe doses of BUP, whose metabolism varies greatly, might differ by up to 5.5 times across individuals consuming the same dosage of the medication (Hesse et al., 2004).

Bupropion hydrochloride (BUP·HCl), is an atypical antidepressant agent, which is increasingly utilized for a range of therapeutic purposes, encompassing smoking cessation, weight management, attention-deficit/hyperactivity disorder (ADHD), seasonal affective disorder (SAD), and amphetamine dependency (Patel et al., 2015; Fava et al., 2005).

Despite its growing acceptance within the medical community, BUP is associated with a recognized challenge, which is the narrow therapeutic margin which might have catastrophic outcomes in cases of overdose (McCabe et al., 2021). It is well documented that its narrow therapeutic window elevate the likelihood of seizures, even within therapeutic dosage ranges (Davidson, 1989; Al-Abri et al., 2013). Despite the importance of maintaining BUP within the therapeutic range, many patients fail to achieve it; recent research findings indicate

* Corresponding author at: Chatham Maritime, Centre for Research Innovation, University of Greenwich, Chatham, Kent ME4 4TB, UK.
** Corresponding author at: Zographou, National and Kapodistrian University of Athens, Athens 157 84, Greece.
E-mail addresses: D.Douroumis@gre.ac.uk (D. Douroumis), vlachou@pharm.uoa.gr (M. Vlachou).

https://doi.org/10.1016/j.ijpharm.2024.124594
Received 9 June 2024; Received in revised form 27 July 2024; Accepted 15 August 2024
Available online 18 August 2024

that BUP, especially the immediate release, emerged as the most lethal antidepressant in the United States (Sheridan et al., 2018; Gummin et al., 2019; Overberg et al., 2019; Steinert and Fröscher, 2018). Therapeutic doses for different patients can vary widely, requiring anywhere between 75 mg up to 522 mg regarding the once-daily dosing form (Saadabadi). Commercially available tablets are manufactured in only a few fixed strengths forms of 12-and 24-h (Saadabadi). Consequently, patients frequently need to utilize a combination of doses, or alternate dosages on different days. This raises the likelihood of patient confusion, medication mistakes, and non-compliance, which could result in serious adverse effects or treatment inefficacy (see Fig. 1).

One of the positives of today's society is the increasing sensitivity towards individuals with special needs, accompanied by a continuous effort to enhance their quality of life. In contrast to the average population, these individuals face an elevated likelihood of experiencing patient safety issues, largely attributed to a heightened vulnerability to medication mistakes (Cupples et al., 2012). Visual impairment (VI) is an international health issue that has an immense effect on an individual's personal, economic, and social life. Recent data state that globally, 1.1 billion people live with vision loss (IAPB Globally, 2020) and 2050, scientists anticipate that 61 million individuals will be blind, 474 million will have moderate and severe VI, 360 million will have mild VI, and 866 million will have uncorrected presbyopia (Bourne et al., 2021). Specifically, about 82 % of blind individuals are 50 years old or older and typically rely on several medications; their visual challenges can influence drug safety and efficacy as they cannot distinguish between drug names and colours. In the realm of aiding such patients, to avoid medication mistakes (Florence and Lee, 2011); recent strategies have predominantly relied on costly audio labelling tools, such as voice-scanning devices and audible monitors as well as an assistance or caregiver (Wasley, 2021; McCann et al., 2012; Awad et al., 2020). The total economic cost of sight loss and blindness in the UK was £28.1 billion in 2013 (Pezzullo et al., 2018). Consequently, this could present a significant issue regarding patient adherence, possibly leading to inadequate medication compliance, which may result in ineffective treatment management, diminished therapeutic effectiveness, and subsequent hospitalizations. Approximately 97 % of visually impaired patients encounter challenges in reading medication labels, even with optical aids, and roughly 24 % have difficulty distinguishing between medications (McCann et al., 2012; Windham et al., 2005). Presently, a method to aid visually impaired patients in identifying medications is by incorporating Braille on medicinal product packaging. However, due to the lack of standardized packaging, patients frequently encounter difficulties in recognizing medications, that may have entirely distinct appearances and tactile sensations, such as varying sizes, shapes, colours of tablets, and packaging. Furthermore, reliance on pharmaceutical packaging for identification becomes less reliable when patients remove the medicine from its original container (McCann et al., 2012).

In general, several advances have been introduced in the medication packages, such as braille patterns on the pillboxes, portable talking medication reminders (Villanueva et al., 2020) and smart medicine planners (Villanueva et al., 2020; Al-Haider et al., 2020). However, to tackle both the issues of visually impaired patients struggling with medication labels and the necessity for personalized dosages of BUP to minimize side effects, it's essential to establish a direct, standardized, and cost-effective approach to integrate Braille patterns directly onto BUP drug products. In this context, three-dimensional (3D) printing could present a sophisticated and pragmatic solution to the issue. 3D printing is an additive manufacturing technique that constructs objects in a layer by layer process (Awad et al., 2020; Douroumis, 2019; Karalia et al., 2021; Nober et al., 2019; Haring et al., 2018; Tagami et al., 2018; Vlachou and Siamidi, 2023).

Specifically, 3D printing is made known in pharmaceutics to provide innovative solutions for challenges encountered by certain patient populations (Awad et al., 2018; Protopapa et al., 2024; Vlachou and Siamidi, 2023). For example, research examining the impact of shape and size on the handling and consuming of 3D printed tablets, revealed that some new designs may be more favourably received compared to traditional shapes (Vlachou et al., 2023; Awad et al., 2022). Additionally, a recent study focusing on paediatric patients with rare metabolic disorder, maple syrup urine disease (MSUD), suggested that 3D printing offers a feasible method for producing customized medications as needed, thereby enhancing the acceptability and effectiveness of treatment (Goyanes et al., 2019). Indicatively, 3D printing has been utilised to produce precise doses of theophylline, a medication with a narrow therapeutic index (TI) commonly used in asthma treatment in order to lower the possibility of drug errors and dose fluctuation (Cheng et al., 2020).

Among the 3D printing techniques, photo-curing or vat polymerization is based on photopolymerization and uses a photosensitive liquid resin, which is cured under light irradiation (Quan et al., 2020). Stereolithography (SLA) is a form of such a 3D printing technology, where the characteristics of the produced tablets are affected by the strength of the light source, scanning speed, exposure period, and amount/type of resin and photoinitiator (Melchels et al., 2010). One of SLA printing's primary advantages is its adaptability; before printing, medications can be combined with the photopolymer and end up immobilised in the solidified composites. The resolution of vat polymerization printers is limited only by the width of the focused laser, and the localized heating, suggesting that the technique is ideal for the manufacture of dosage forms with thermally labile drugs (Melchels et al., 2010). Another newly introduced vat polymerization printing technique is the liquid crystal

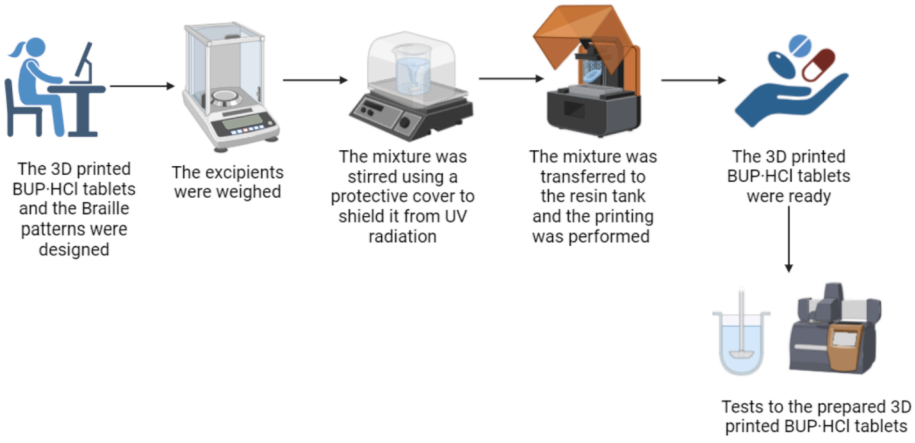

Fig. 1. The methodology for producing the 3D BUP tablets with Braille patterns; created using BioRender.com https://www.biorender.com/ (accessed on 15 April 2024).

display (LCD), where the UV light is produced by light-emitting diodes (LEDs) (Madžarević and Ibrić, 2021). Ultraviolet (UV) light wavelengths are often used by LCD printers, but lately, visible light (405 nm) has been found to induce photopolymerization in LCD projectors.

In this research, an LCD 3D printer was used to develop printed tablets with Braille patterns, in order for patients to recognise BUP drugs by these sensory characteristics, particularly if they were removed from the original package.

2. Materials and methods

The active ingredient BUP·HCl in the form of its hydrochloride salt, was kindly donated by Gattefossse (Lyon, France). The excipients PEG200, Tween 80, poly(ethylene glycol) (PEG)-diacrylate (PEGDA400), and the photoinitiator phenyl-bis(2,4,6-trimethylbenzoyl) phosphine oxide (TPO) were purchased from the Tokyo Chemical Ltd. (Tokyo, Japan). The PEGDA700 resin was purchased from Sigma-–Aldrich Ltd. (Steinheim, Germany).

2.1. Three-Dimensional printing

PEGDA served as the photopolymerizable monomer, while TPO was used as the photoinitiator (PI). Each formulation (Table 1) was prepared by dissolving BUP·HCl in water, under continuous stirring, at ambient temperature. Then, a carefully selected combination of excipients, including PEG200, Tween80, and either PEGDA700 or PEGDA400, were cautiously incorporated into the stirred solution. The resulting mixture was stirred for 10 more min to ensure uniformity. TPO was then added into each formulation, under stirring, for approximately 2 h or until TPO was fully dissolved. To safeguard against polymerization and premature solidification, a protective cover was used, shielding the mixture from UV radiation. The prepared mixture was then poured into resin trays, primed for the subsequent printing processes.

All printed tablets were prepared using an LCD 3D printer (Creality, Shenzhen, China). The printer was furnished with a 405 nm laser capable to develop objects with a resolution accuracy of 0.034 mm, a layer thickness of 0.01–0.2 mm and a printing speed of 1–4 s/layer. The Duxbury Braille translator Win 12.7 SR2, 2023 was used to translate the word BUP (referring to bupropion) into Braille pattern. The printed tablets of x = 10 mm y = 10 mm z = 5.2 mm with the Braille pattern on them x = 0.7 mm, y = 0.7 mm and z = 0.5 mm, were created using AutoCAD® 2023 software from Autodesk Inc., located in San Rafael, CA, USA, was used to design the tablets, which were then saved in stereolithographic format (.stl). These tablets were fabricated directly onto the build platform at ambient temperature, without the need for any additional supports. Following printing, the tablets were rinsed with deionized water, gently dried with filter paper to eliminate any excess uncured liquid formulation, and subsequently exposed to UV light for an additional 2 min to ensure thorough polymerization.

2.2. Tablets' physical characteristics and breaking force

The weight and dimensions (both width and height) of the tablets were evaluated using a precise 4-digit scale and a Vernier calliper, respectively. Each measurement was performed three times to guarantee precision.

The breaking forces of ten tablets were determined using a tablet hardness tester (TBH 28, Erweka GmbH, Heusenstamm, Germany). Increased tension was incrementally exerted, perpendicularly to the tablet axis on its opposing sides until it cracked.

Table 1
Shows the compositions of the developed formulations.

Material	Formulation					
	F1 (% w/w)	F2 (% w/w)	F3 (% w/w)	F4 (% w/w)	F5 (% w/w)	F6 (% w/w)
BUP·HCl	2.5	2.5	2.5	2.5	2.5	2.5
PEGDA400	28.2	28.2	28.2	–	–	–
PEGDA700	–	–	–	28.2	28.2	28.2
PEG200	–	28.3	56.6	–	28.3	56.6
Tween80	56.6	28.3	–	56.6	28.3	–
H_20	11.7	11.7	11.7	11.7	11.7	11.7
TPO	1	1	1	1	1	1

2.3. X-ray powder diffraction (XRPD)

The X-ray powder diffraction patterns of previously pulverized printed tablets (23 × 1 mm) and bulk BUP·HCl were captured utilizing a LynxEye silicon strip detector and a D8 Advance diffractometer (Bruker, Billerica, MA, USA) with Cu Kα radiation (40 kV, 40 mA). Data collection ranged from 3 to 40° 2θ at a rate of 2° per minute, employing a step size of 0.02° and a counting time of 0.3 s per step. Voltage and intensity settings of 40 kV and 15 mA were utilized. The angular range for data acquisition was 3–40° 2θ.

2.4. Differential scanning calorimetry (DSC)

Thermal analysis of the BUP·HCl was carried out using a DSC-3 (Mettler Toledo, Switzerland). Samples (4–5 mg each) of pulverized tablets were precisely weighed in aluminum pans and hermetically sealed with lids. Tests were performed on pure BUP·HCl and six different formulations. Thermograms were recorded from 25 °C to 250 °C at a heating rate of 10 °C per minute, with a nitrogen gas flow rate of 20 mL/min. An empty aluminum pan served as the reference.

2.5. Thermal gravimetric analysis (TGA)

Thermal gravimetric analysis of BUP·HCl was carried out using a TGA Q5000 (Thermal Instruments, Moraine, OH, USA). Temperature measurements were recorded from 25 °C to 350 °C at a heating rate of 10 °C per minute.

2.6. SEM pictures

To assess the Braille imprinted patterns on the tablet morphology, scanning electron microscopy (SEM) (Hitachi SU8030, Japan) was utilized. The SEM pictures of the 3D printed tablet sections were taken at 36- and 38-times magnification, respectively, using an electron beam accelerator voltage of 2 kV.

2.7. Determination of drug concentration

For the determination of drug concentration, the printed tablets were ground into a fine powder using a mortar and pestle. The amount of powder equivalent to the mass of a single tablet was then dissolved in 1 L of deionized water, with continuous stirring provided by a magnetic stirrer for 24 h. The resultant solution was filtered through 0.45 μm pore size filters (Millipore Ltd., Dublin, Ireland). The drug concentration in the filtered solution was measured with a UV–VIS spectrophotometer (uniSPEC 2 Spectrophotometer, LLG Labware, Meckenheim, Germany) at a wavelength of 251 nm (λmax). To ensure accuracy, the measurements were performed three times.

2.8. Dissolution studies

The release of BUP·HCl from each formulation was assessed using a USP II dissolution paddle apparatus (PharmaTest-D17, Hainburg, Germany) at 50 rpm and a temperature of 37 ± 0.5 °C. For the first 2 h, a pH 1.2 aqueous medium (450 mL) was employed to mimic the stomach environment, and to that, 450 mL of 0.14 M K_2HPO_4 solution (pH 9) was added to simulate the enteric pH (pH 6.8). after which a pH 6.8 aqueous solution was used to replicate the small intestine environment. At

predetermined intervals, 5 mL samples from each medium were collected, filtered through 0.45 μm pore size filters (Millipore Ltd., Ireland), and analyzed with a UV–VIS spectrophotometer (uniSPEC 2 Spectrophotometer LLG Labware, Meckenheim, Germany) at λmax = 251 nm. These dissolution tests were repeated three times, resulting in graphs that show the percentage release (mean ± SD) over time.

2.9. Mathematical and statistical analysis

The data collected from the dissolution studies were fitted to release kinetics including first- and zero-order, Higuchi and Korsmeyer–Peppas equations, using the GraphPad Prism 8 (version 5.01) software (Peppas et al., 1987; Costa and Lobo, 2000).

2.10. Determination of swelling ratio (SR)

The printed tablets for each formulation were weighed (Md), then placed into 50 ml of pH 1.2 aqueous medium for the first 2 h, and then, into a 50 ml pH 6.8 aqueous medium for 22 h at 37 ± 0.5 °C to simulate the dissolution test conditions. During the initial two-hour period, the tablets were weighed every half-hour, while for the subsequent six hours, they were weighed every hour. In all cases the excess water was carefully wiped off before weighing (Ms). The SR was calculated using the following equation:

$$SR = \frac{Ms - Md}{Md} \quad (1)$$

3. Results and discussion

3.1. Printing process

In this study, the LCD 3D printing process was effectively employed to imprint Braille patterns onto the surface of cylindrical printed tablets. The LCD printer presents a notable advantage in its accessibility, as it requires no specialized skills from the operator for the preparation and printing of tablets. However, it is crucial to acknowledge a key drawback: the photosensitivity of the mixture. Operators must exercise caution to shield the mixture from UV radiation to prevent premature solidification. The scope of this work was to develop personalized solid oral, tailor-made BUP·HCl dosage forms, specifically for individuals who are blind or visually impaired. Pictures of the printed tablets are presented in Fig. 2, which effectively showcased the capability of LCD 3D printing to create tablets with intricate and complex patterns. This development could help visually impaired patients become more independent and adhere to their prescription regimens.

Recently, researchers have also printed customized tablets and buccal films with Braille and Moon patterns for the VI patients (Awad et al., 2020; Eleftheriadis and Fatouros, 2021). This groundbreaking alternative has emerged in the form of innovative 3D-printed dosage forms featuring Braille patterns. These printed tablets offer a practical and cost-effective solution, as they can be swiftly manufactured in a single step, obviating the need for additional equipment or procedures and facilitating medication recognition for patients. After the addition of the formulation into the resin tray, adaptations were made to the printer's operational settings. The parameters governing the printing process are shown in Table 2.

The manufacture of the printed tablets, as depicted in Fig. 2, required only 24 min. Notably, the resulting tablets featured well-defined shapes, with Braille patterns noticeable both visually and with tactile recognition. The printed patterns were verified by a blind member of the Panhellenic Society of the Visually Impaired. The efficiency of the printing process was further highlighted by the ability to print approximately 63 tablets simultaneously on the building platform, as illustrated in Fig. 2**b**. This advancement holds significant promise, particularly for visually impaired individuals, who could effortlessly produce their personalized medication in advance for a significant period of time within a brief span of 24 min.

Table 2 illustrates the optimized printing parameters after various modifications to produce robust tablets in terms of hardness and

Table 2
Printing parameters.

Parameters	Values
Layer Thickness	0.050 mm
Initial Exposure	40 s
Exposure Time	3 s
Rising high	8 mm
Motor speed	5 mm/s
Turn off Delay	4 s
Bottom Exposure layer	2

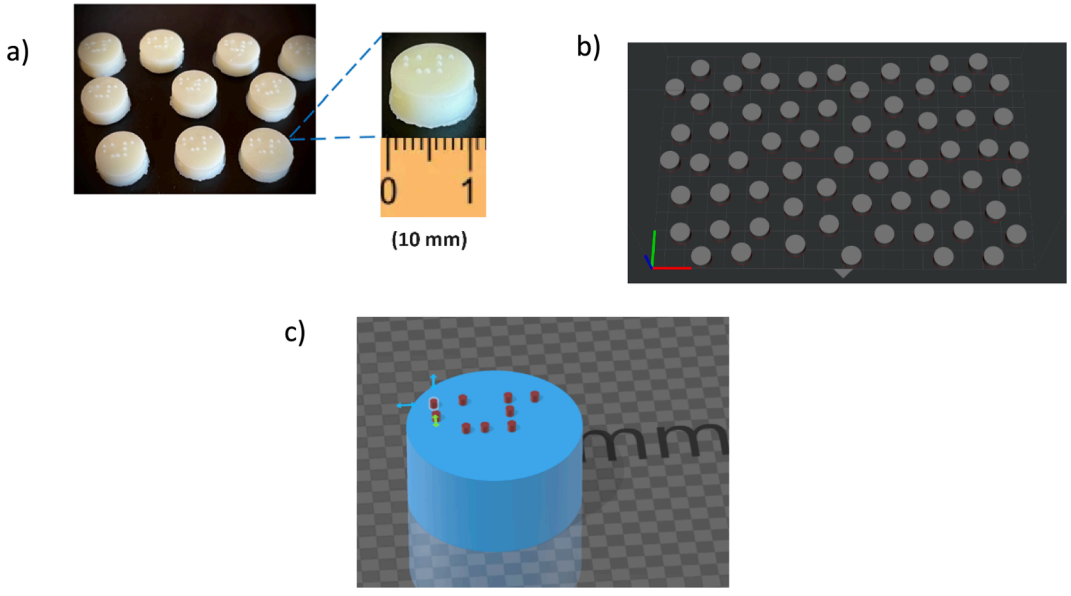

Fig. 2. A) optical image of bup·hcl printed tablets with braille patterns, b) scalability of printed tablets for simultaneous manufacture of 63 tablets and c) design of 3d printed tablets with the braille patterns.

friability including high printing accuracy throughout the process. In general, PEGDA has been extensively used in many biomedical applications due to its cytocompatibility, lack of toxicity, and ease of use (Mazzoccoli et al., 2010; Cruise et al., 1998; Hahn et al., 2006). A lot of researches have used PEGDA for the preparation of oral delivery formulations (Madžarević and Ibrić, 2021; Adamov et al., 2022; Chen et al., 2022; Kadry et al., 2019; Krkobabić et al., 2019; Pariskar et al., 2023; Robles-Martinez et al., 2019; Wang et al., 2016). However, until today there is not any toxicological research that certifies its safe and non-toxic effect on the body after *per os* administration. In this research, two PEGDA excipients with different molecular mass were used, the PEGDA400 and PEGDA700. The increase in the molecular weight of the PEGDA affects the BUP·HCl release rate and the swelling ratio (*vide infra*).

The other two excipients, PEG200 and Tween 80 were used at different ratios to control the release of the BUP·HCl from the printed tablets. When both excipients are used in combination with PEGDA, they disrupt the complete polymerization process. Specifically, where the excipients are present in the mixture, polymerization is interrupted, resulting in the formation of holes. These holes facilitate the dissolution and release of the drug into the dissolution media.

3.2. Tablets' physical characteristics

The tablets' weights and diameters were measured in order to assess them: x = 10 mm, y = 10 mm, z = 5.2 mm) (Table 3). When assessing the width, height, and weight, the recorded differences among the six formulations remained in line with the initial inputs of the printing process. The mechanical characteristics of the tablets, whether with or without Braille patterns, were evaluated (Table 3). Incorporating the patterns showed no impact on the tablets' mechanical properties, as all of them exhibited comparable hardness. The formulations containing PEGDA400 exhibited higher breaking force values compared to the formulations containing PEGDA700. This is because the higher molecular mass of PEGDA clearly reduced the quantity of free acrylate groups, which are capable of creating covalent crosslinks leading to a reduced crosslinking degree and greater elastic response of the PEGDA chains (Rekowska et al., 2023).

3.3. Physicochemical characterisation for 3D printed tablets

Thermogravimetric analysis (TGA) carried out over a temperature range from 25 °C to 350 °C to investigate the BUP thermal stability. As shown in Fig. 3, it was observed that 96 % of the drug remained intact up to 170 °C.

The melting point of BUP·HCl generally ranges from 170 °C to 233 °C. However, at 233 °C, BUP·HCl underwent thermal degradation or decomposition, with 95.85 % degradation observed. In all six formulations, the printing was performed at room temperature, where no BUP·HCl degradation takes place, according to the TGA findings.

Further analysis included the use of DSC to investigate the physical state of BUP in the printed tablets. As shown in Fig. 4 the bulk BUP presented a melting endotherm at 240 °C followed by a sharp exothermic peak at 256 °C related to the initiation of drug degradation. For all the 3D printed tablets, BUP appeared to be in the amorphous state, due to the absence of the melting endotherm. This is a strong indication of the solubilizing capacity of the used excipients for BUP.

Further investigation was conducted by using XRPD analysis for the 3D printed tablets. As shown in Fig. 5, no BUP diffraction peaks could be observed for the printed dosage forms. The results confirmed the DSC observations that BUP is probably molecularly dispersed in the printed structures.

Table 3
Dimensions, weights and breaking forces of the printed tablets (n = 10).

Formulations	Width (mm)	Height (mm)	Weight (mg)	Hardness (N)
F1	10 ± 0.43	5.2 ± 0.243	405 ± 2.04	6.32 ± 0.58
F2	10 ± 0.39	5.2 ± 0.312	406 ± 3.12	6.69 ± 0.74
F3	10 ± 0.49	5.2 ± 0.210	405 ± 3.24	6.02 ± 0.52
F4	10 ± 0.41	5.2 ± 0.102	404 ± 3.65	2.60 ± 0.22
F5	10 ± 0.36	5.2 ± 0.210	405 ± 3.21	2.6 ± 0.50
F6	10 ± 0.39	5.2 ± 0.300	406 ± 2.10	3.38 ± 0.08

3.4. SEM analysis

SEM imaging analysis was used to visualize the microstructure surface morphology and the formation of the Braille patterns after photopolymerization. As illustrated in Fig. 6, the Braille patterns on the surface of the tablets were well structured, allowing for tactile identification, as previously stated. It can also be observed that the presence of other excipients, aside from PEGDA, creates pores that interrupt the full polymerization process of PEGDA, as previously mentioned. This interruption provides the opportunity for the drug to dissolve and be released from the tablet.

3.5. Dissolution studies

For all the printed tablets developed in the context of this work, the estimated drug content was expressed as a percentage of target drug content. Results ranged between 99.4 to 102.8 % drug content and fall within the proxy USP standard percentage range.

Surface morphology evaluation of the developed 3D printed tablets was conducted using SEM images both before and after swelling, although this data is not presented here. The SEM analysis revealed that the "dry" tablets displayed a compact surface due to monomer cross-linking within the polymeric matrix. Conversely, numerous pores were observed on the surface of swollen tablets when exposed to the dissolution medium. These findings emphasize that the mechanism of drug release from the LCD printed tablets involves water diffusion into the tablet, followed by the release of the drug through micropore channels within the printed structure.

The study by Robles-Martinez *et al.* examined the release of six different active ingredients from a six-layered tablet, printed using an SLA 3D printer (Robles-Martinez et al., 2019). It was observed that the poor aqueous solubility and the affinity of the drug to the polymer can influence its release from the 3D-printed tablets. In our case, however, as BUP·HCl is hydrophilic, its physicochemical characteristics do not affect the drug release in any way.

In previous researches from Wang et al. and Robles-Martinez et al., the drug release was not 100 %, likely due to incomplete drug extraction from the cross-linked printed tablet (Wang et al., 2016; Martinez et al., 2018). However, in this research, BUP·HCl was fully released in all six formulations after 480 min. This can be attributed to the fact that BUP·HCl fully dissolves in water rather than in PEGDA, which could limit its release.

As depicted in Fig. 7, all six formulations of the printed BUP·HCl tablets showed sustained release profiles. During the first 2 h, at pH = 1.2, the release rates varied from 48 to78 % depending on the tablet composition. The tablets comprising of PEGDA-400 presented faster release rates (69–78 %) compared to the PEGDA-700 (48–50 %). Despite the low hardness values of PEGDA700 (2.5–3.4 N) the higher molecular weight of the polymer affected the dissolution rates, due to the higher cross linking that PEGDA700 induces compared with the PEGDA400. The higher the crosslinking, the harder for the drug is to escape and dissolve to the dissolution media. In addition, the presence of surfactants (Tween 80) or solubilizers (PEG200) were among the critical material attributes that influence the BUP release rates. As it can be seen in Table 3, the addition of Tween 80, a non-ionic surfactant (HLB = 15) resulted in faster dissolution rates for both polymers (F1, F4). For tablets with both Tween 80 and PEG200, the release rates were slightly lower. The slowest dissolution rates were observed when only PEG200 was

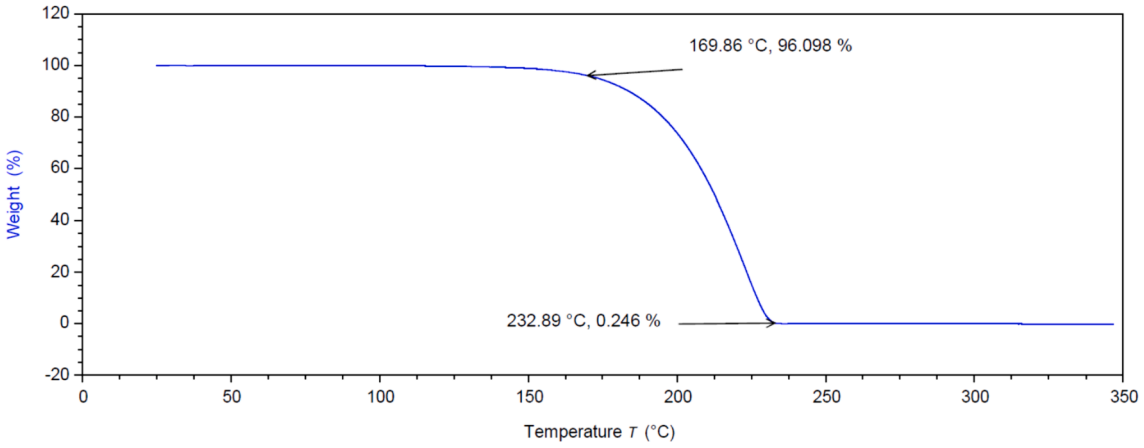

Fig. 3. Thermal Gravimetric Analysis.

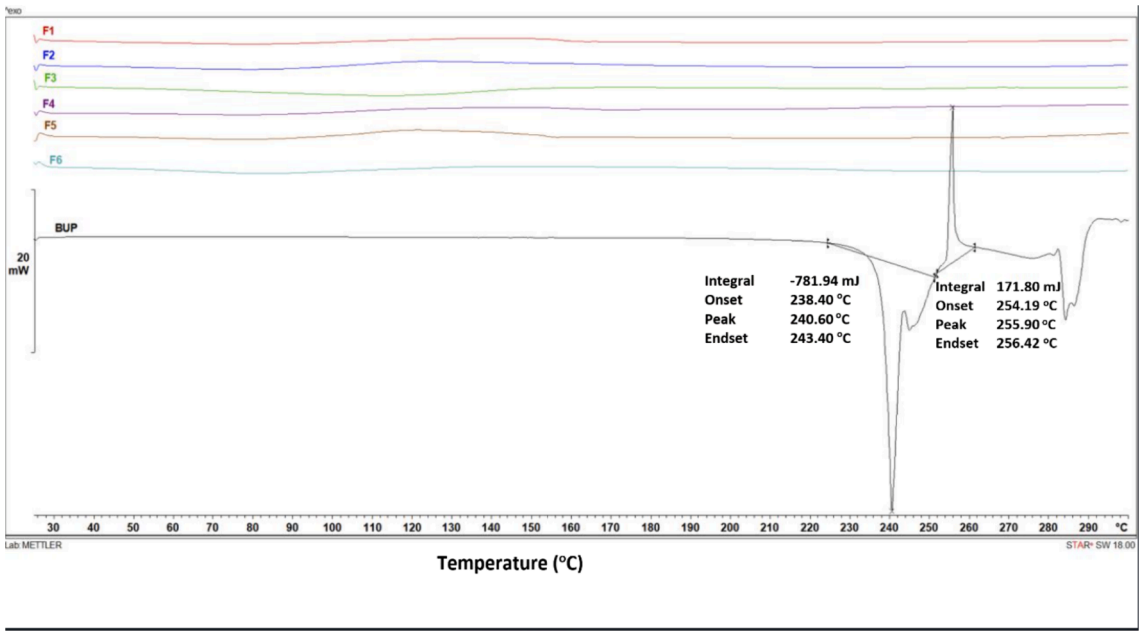

Fig. 4. DSC thermograms of bulk BUP and 3D printed tablets.

used in the tablet formulations for both polymers (F4, F6). Overall, the addition of high amounts of surfactant or solubilizer facilitated faster dissolution rates.

From these results it becomes apparent that the dissolution rates can be tuned by altering the formulation composition and more specifically by adjusting the ratio of Tween80 to PEG200. Hence, by modifying the composition of the printable inks, the BUP dissolution profiles can match those of the marketed products. Overall, drug molecule release behaviour from 3D printed structures is generally complicated and dependent on several variables. Higher molecular mass (e.g., PEGDA700) typically results in increased swelling, decreased cross-linked density, and enhanced polymer-water interactions—all of which increase release rates. Nonetheless, it is common for PEGDA with a smaller molecular mass to facilitate faster dissolution rates for various molecules (e.g., proteins). This has been linked to PEGDA700′s increased viscosity or possible interactions with other excipients like PEG200 or Tween 80, which can reduce the formation of covalent bods.

Another interesting observation is that tablets remained intact and did not dissolve after 8 h in the media, as shown in Fig. 7 (inset). This is due to the strong covalent bonds formed during crosslinking of the polymerized resin which prevent the tablet dissolution process. This behaviour has been observed in other sustained release systems, when lipids are used as the main tablet component (Vithani et al., 2013; Vithani et al., 2014).

To the best of our knowledge, this is the first time that BUP·HCL has been used for the development of 3D printed tablets with controlled release rates. In general, photocuring 3D printing technologies have been utilized extensively in pharmaceutics. For example, several studies demonstrated the printing of modified release formulations with SLA 3D printer (Kadry et al., 2019; Krkobabić et al., 2019; Wang et al., 2016; Rodríguez-Pombo et al., 2023; Rodríguez-Pombo et al., 2022). Similarly other groups have used SLA 3D printing to create hydrogels loaded with ascorbic acid (Karakurt et al., 2020) and multilayer (up to 6 layers) polypills (Robles-Martinez et al., 2019; Rodríguez-Pombo et al., 2023). However, the newer technology LCD that is used in this research has not been exploited, as yet, in terms of printing pharmaceutical dosage forms and scale-up of small batches. Madzarevic and Ibric, used a LCD printer application for the fabrication of ibuprofen extended release tablets (Madžarević and Ibrić, 2021).

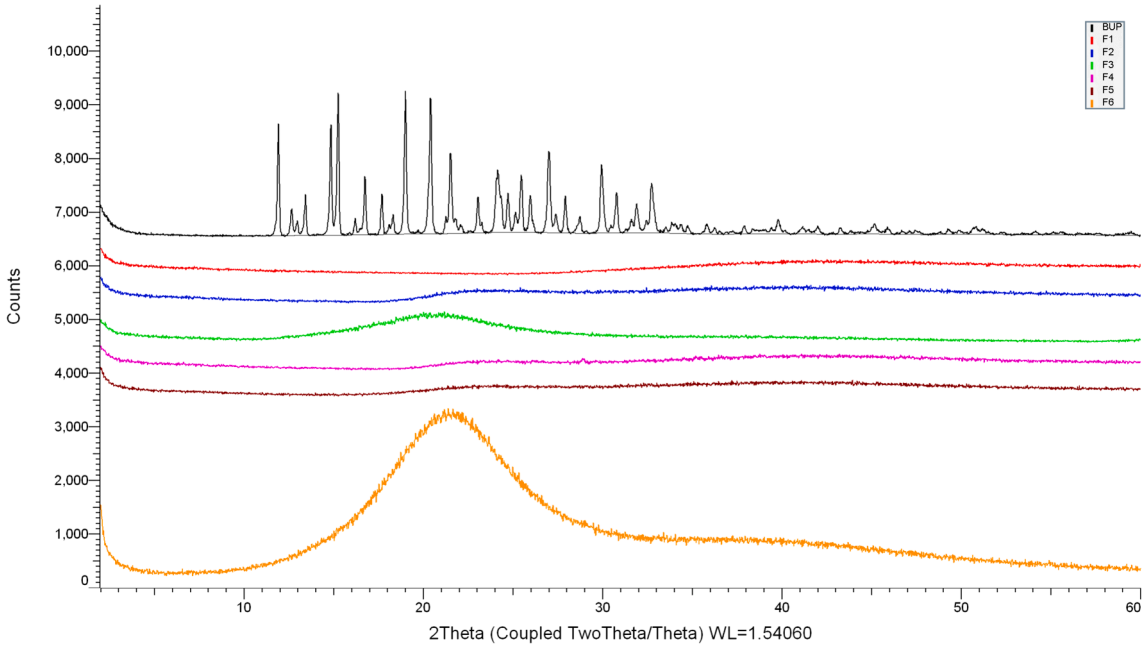

Fig. 5. X-Ray Powder Diffraction.

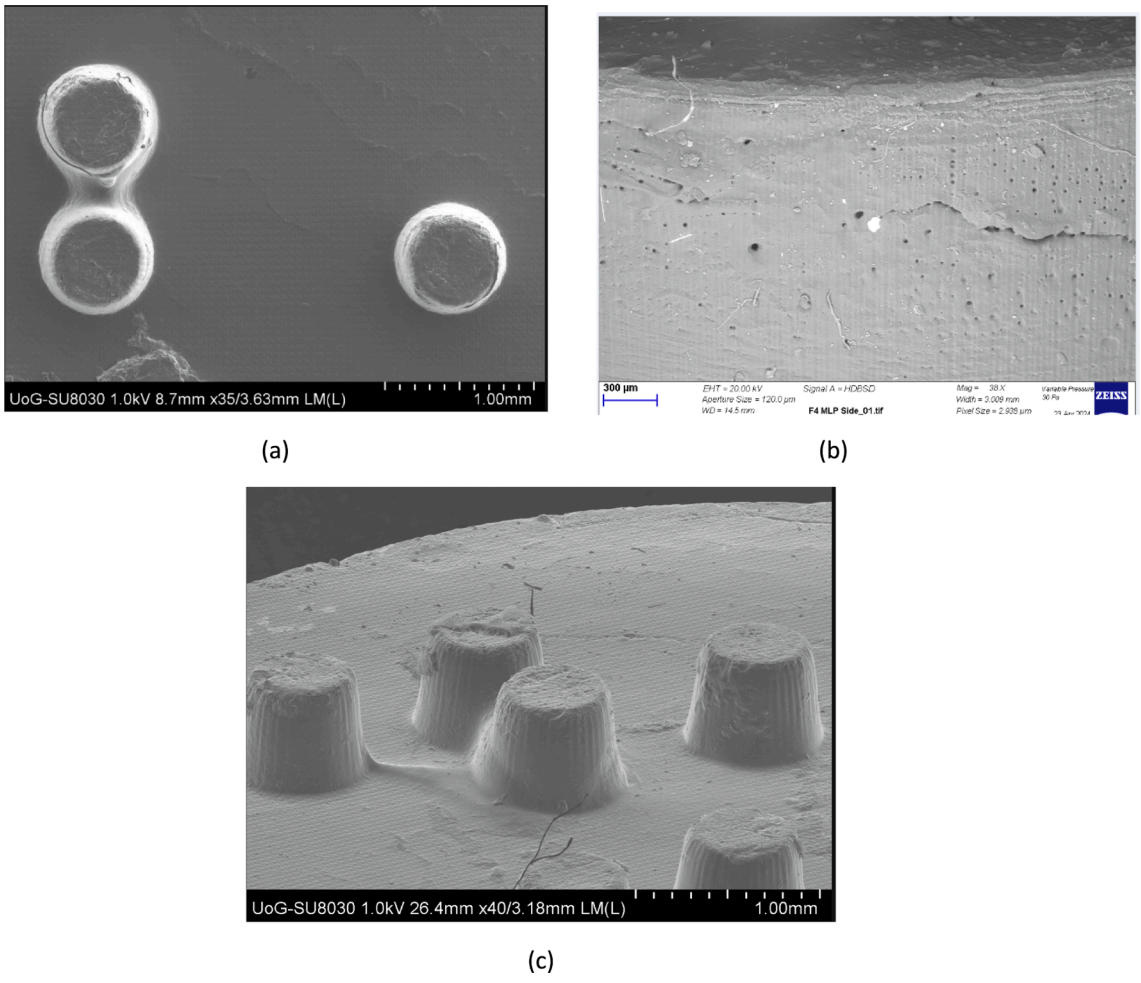

Fig. 6. SEM figures of MLT 3D printed tablets showing the Braille imprints: (a) Top view, magnification x35 (b) Side view of the surface, magnification X38; (c) Side view, magnification X40.

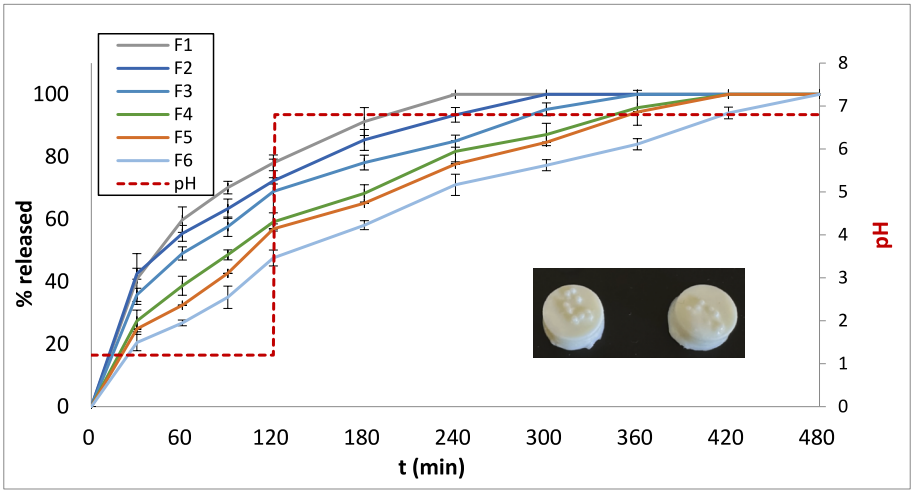

Fig. 7. Dissolution profiles of BUP·HCl of 3D printed tablets at pH 1.2 (0–120 min) and at pH 6.8 (120–480 min). Results represent the mean value (n = 3, SD < 2). Inset: 3D printed tablets after 8 h of dissolution.

3.6. BUP release kinetics

Table 4 illustrates the release kinetics of BUP·HCl from the 3D printed formulations. Evidently, in most cases, the release mechanism follows the Higuchi model, except from the F2 formulation, where the Korsmeyer–Peppas mechanism is predominant (Costa and Lobo, 2000).

Concerning the *n* value of the Korsmeyer–Peppas equation, it can be concluded that from the F1-F3 formulations, the BUP·HCl's release follows the Fickian diffusion model ($n \leq 0.45$), while from the F4, F5 an anomalous diffusion release is followed ($0.45 \leq n \leq 0.89$).

3.7. Determination of swelling ratio (SR)

As shown in Table 5 the swelling ratio, was monitored over 24 h, until a maximum swelling ratio was reached. The findings indicate that the formulations containing PEGDA400 exhibited lower swelling ratios compared to those containing PEGDA700. Within each group of formulations, F1-F3 (containing PEGDA400), and F4-F6 (containing PEGDA700), the formulation with the highest swelling ratio was observed in the presence of Tween 80, followed by the formulations with combined Tween 80 and PEG200, while those with only PEG200 presented the lowest swelling capacity. This phenomenon can be attributed to the interaction of Tween 80 with the aqueous media, resulting in a spindle-shaped ellipsoid structure that enhances swelling (Karjiban et al., 2012). Also, when the PEG200 concentration is lower, there is a preference for molecular structure cyclization, resulting in a less rigid and more porous framework that exhibits increased swelling capacity (Della Sala et al., 2020).

In addition, the molecular weight of PEGDA plays a significant role in the swelling ratio (Table 2). It is highly probable that the increased molecular mass noticeably reduced the availability of free acrylate groups, which play a role in forming covalent crosslinks. Consequently, this led to a reduced level of crosslinking and an enhanced elastic response of the PEGDA chains, along with an increased capacity for water absorption (Della Sala et al., 2020; Karoyo and Wilson, 2021). The molecular weight, length, and mobility of the monomer chains play significant roles in photopolymerization and consequently impact the resulting degree of crosslinking (Ju et al., 2009). Longer chains typically exhibit more limited mobility, with mobility further decreasing during the photopolymerization process, which impedes the migration of chains towards radical groups (Peris et al., 2012). This phenomenon contributes to a reduction in the formation of covalent crosslinks and an expansion in mesh size, thereby enhancing water uptake.

Table 5
Maximum swelling ratios of the printed tablets within 24 h in aqueous media.

Formulation	Maximum swelling ratio	Swelling ratio (*) (h)
F1	0.37 ± 0.02	3
F2	0.14 ± 0.01	2
F3	0.12 ± 0.02	2
F4	0.79 ± 0.01	6
F5	0.56 ± 0.02	24
F6	0.51 ± 0.01	24

* Time when maximum swelling ratio was reached.

4. Conclusions

LCD printing technology was introduced for the development of personalised BUP tablets with Braille patterns for blind or visually impaired patients. The composition of printing inks including PEGDA of different molecular weights, and the presence of solvents or surfactants were found to be the key factors for achieving sustained drug release rates for over 8 h. The disrupting of the PEGDA photopolymerisation allowed complete dissolution rates without drug entrapment in the

Table 4
Drug release mechanisms for the 3D-printed tablets.

Formulation	Zero order			First order		Higuchi		Korsmeyer Peppas		
	R^2	Y_0	K_0	R^2	Y_1	R_2	K_H	R^2	K_{HP}	*n*
F1	0.93	41.60	0.27	0.88	48.48	**0.95**	6.92	0.92	9.15	0.45
F2	0.95	43.03	0.21	0.91	49.01	0.91	6.26	**0.98**	11.08	0.39
F3	0.94	39.32	0.19	0.89	45.98	**0.95**	5.64	0.94	9.27	0.41
F4	0.95	31.12	0.18	0.89	39.87	**0.99**	5.07	0.98	4.68	0.52
F5	0.96	25.95	0.19	0.90	35.84	**0.99**	4.82	0.97	4.08	0.53
F6	0.97	21.23	0.18	0.90	32.20	**0.99**	4.43	0.98	2.59	0.60

resin. The LCD printing technology offers significant advantages for scaling-up manufacturing, due to the fast-printing times of small batches, thus meriting praise for further studies.

CRediT authorship contribution statement

Chrystalla Protopapa: Writing – review & editing, Writing – original draft, Software, Investigation, Formal analysis, Data curation. **Angeliki Siamidi:** Writing – review & editing, Writing – original draft, Validation, Software, Investigation, Formal analysis, Data curation. **Laura Andrade Junqueira:** Software, Methodology, Investigation, Formal analysis, Data curation. **Siva Kolipaka:** Software, Investigation, Formal analysis, Data curation. **Atabak Ghanizadeh Tabriz:** Visualization, Software, Methodology, Conceptualization. **Dennis Douroumis:** Writing – review & editing, Writing – original draft, Visualization, Supervision, Resources, Project administration, Methodology, Investigation, Data curation, Conceptualization. **Marilena Vlachou:** Writing – review & editing, Writing – original draft, Visualization, Supervision, Resources, Project administration, Funding acquisition.

Declaration of competing interest

The authors declare that they have no known competing financial interests or personal relationships that could have appeared to influence the work reported in this paper.

Data availability

Data will be made available on request.

Acknowledgments

The research work was supported by the Hellenic Foundation for Research and Innovation (HFRI) under the 5th Call for HFRI PhD Fellowships grant to C.P. (Fellowship Number: 20610).

References

Adamov, I., Stanojević, G., Medarević, D., Ivković, B., Kočović, D., Mirković, D., Ibrić, S., 2022. Formulation and characterization of immediate-release oral dosage forms with zolpidem tartrate fabricated by digital light processing (DLP) 3D printing technique. Int. J. Pharm. 624 https://doi.org/10.1016/j.ijpharm.2022.122046.

Al-Abri, S.A., Orengo, J.P., Hayashi, S., Thoren, K.L., Benowitz, N.L., Olson, K.R., 2013. Delayed bupropion cardiotoxicity associated with elevated serum concentrations of bupropion but not hydroxybupropion. Clin. Toxicol. 51, 1230–1234. https://doi.org/10.3109/15563650.2013.849349.

Al-Haider, A.J.; Al-Sharshani, S.M.; Al-Sheraim, H.S.; Subramanian, N.; Al-Maadeed, S.; Chaari, M.Z. Smart Medicine Planner for Visually Impaired People. In: *2020 IEEE Int. Conf. Informatics, IoT, Enabling Technol. ICIoT 2020* **2020**, 361–366, doi:10.1109/ICIoT48696.2020.9089536.

Awad, A., Basit, A.W., Alvarez-lorenzo, C., Goyanes, A., 2022. Innovations in Chewable Formulations : The Novelty and Applications of 3D Printing in Drug Product Design.

Awad, A., Trenfield, S.J., Goyanes, A., Gaisford, S., Basit, A.W., 2018. Reshaping drug development using 3D printing. Drug Discov. Today 23, 1547–1555. https://doi.org/10.1016/j.drudis.2018.05.025.

Awad, A., Yao, A., Trenfield, S.J., Goyanes, A., Gaisford, S., Basit, A.W., 2020. 3D printed tablets (Printlets) with braille and moon patterns for visually impaired patients. Pharmaceutics 12, 1–14. https://doi.org/10.3390/pharmaceutics12020172.

Bourne, R.R.A., Steinmetz, J.D., Flaxman, S., Briant, P.S., Taylor, H.R., Resnikoff, S., Casson, R.J., Abdoli, A., Abu-Gharbieh, E., Afshin, A., et al., 2021. Trends in prevalence of blindness and distance and near vision impairment over 30 years: An analysis for the Global Burden of Disease Study. Lancet Glob. Heal. 9, e130–e143. https://doi.org/10.1016/S2214-109X(20)30425-3.

Breitkreutz, J., Boos, J., 2007. Paediatric and geriatric drug delivery. Expert Opin. Drug Deliv. 4, 37–45. https://doi.org/10.1517/17425247.4.1.37.

Peek, Brian T., Antoine Al-Achi, S.J.C., 2015. Accuracy of tablet splitting by elderly patients. **2015**.

Chen, K.Y., Zeng, J.J., Lin, G.T., 2022. Fabrication of 5-fluorouracil-loaded tablets with hyperbranched polyester by digital light processing 3D printing technology. Eur. Polym. J. 171, 111190 https://doi.org/10.1016/j.eurpolymj.2022.111190.

Cheng, Y., Qin, H., Acevedo, N.C., Jiang, X., Shi, X., 2020. 3D printing of extended-release tablets of theophylline using hydroxypropyl methylcellulose (HPMC) hydrogels. Int. J. Pharm. 591, 119983 https://doi.org/10.1016/j.ijpharm.2020.119983.

Costa, P., Lobo, J.M.S., 2000. Modeling and comparison of dissolution profiles of diltiazem modified-release formulations. Eur. J. Pharm. Sci. 13, 123–133. https://doi.org/10.14227/DT160209P41.

Cruise, G.M., Scharp, D.S., Hubbell, J.A., 1998. Characterization of permeability and network structure of interfacially photopolymerized poly(ethylene glycol) diacrylate hydrogels. Biomaterials 19, 1287–1294. https://doi.org/10.1016/S0142-9612(98)00025-8.

Cupples, M.E., Hart, P.M., Johnston, A., Jackson, A.J., 2012. Improving healthcare access for people with visual impairment and blindness. BMJ 344. https://doi.org/10.1136/bmj.e542.

Davidson, J., 1989. Seizures and bupropion: a review. J. Clin. Psychiatry 50, 256–261.

Della Sala, F., Biondi, M., Guarnieri, D., Borzacchiello, A., Ambrosio, L., Mayol, L., 2020. Mechanical behavior of bioactive poly(ethylene glycol) diacrylate matrices for biomedical application. J. Mech. Behav. Biomed. Mater. 110, 103885 https://doi.org/10.1016/j.jmbbm.2020.103885.

Douroumis, D., 2019. 3D printing of pharmaceutical and medical applications: a new era. Pharm. Res. 36 https://doi.org/10.1007/s11095-019-2575-x.

Eleftheriadis, G.K., Fatouros, D.G., 2021. Haptic Evaluation of 3D-printed Braille-encoded Intraoral Films. Eur. J. Pharm. Sci. 157, 105605 https://doi.org/10.1016/j.ejps.2020.105605.

Fava, M., Rush, A.J., Thase, M.E., Clayton, A., Stahl, S.M., Pradko, J.F., Johnston, J.A., 2005. 15 Years of clinical experience with bupropion HCl: From bupropion to bupropion SR to bupropion XL. Prim. Care Companion J. Clin. Psychiatry 7, 106–113. https://doi.org/10.4088/pcc.v07n0305.

Florence, A.T., Lee, V.H.L., 2011. Personalised medicines: More tailored drugs, more tailored delivery. Int. J. Pharm. 415, 29–33. https://doi.org/10.1016/j.ijpharm.2011.04.047.

Goyanes, A., Madla, C.M., Umerji, A., Duran Piñeiro, G., Giraldez Montero, J.M., Lamas Diaz, M.J., Gonzalez Barcia, M., Taherali, F., Sánchez-Pintos, P., Couce, M.L., et al., 2019. Automated therapy preparation of isoleucine formulations using 3D printing for the treatment of MSUD: First single-centre, prospective, crossover study in patients. Int. J. Pharm. 567, 118497 https://doi.org/10.1016/j.ijpharm.2019.118497.

Gummin, D.D., Mowry, J.B., Beuhler, M.C., Spyker, D.A., Brooks, D.E., Dibert, K.W., Rivers, L.J., Pham, N.P.T., Ryan, M.L., 2019. Annual report of the American association of poison control centers' national poison data system (NPDS): 37th annual report. Clin. Toxicol. (phila) 2020 (58), 1360–1541. https://doi.org/10.1080/15563650.2020.1834219.

Hahn, M.S., Miller, J.S., West, J.L., 2006. Three-dimensional biochemical and biomechanical patterning of hydrogels for guiding cell behavior. Adv. Mater. 18, 2679–2684. https://doi.org/10.1002/adma.200600647.

Haring, A.P., Tong, Y., Halper, J., Johnson, B.N., 2018. Programming of multicomponent temporal release profiles in 3D printed polypills via core-shell, multilayer, and gradient concentration profiles. Adv. Healthc. Mater. 7, 1–10. https://doi.org/10.1002/adhm.201800213.

Hesse, L.M., He, P., Krishnaswamy, S., Hao, Q., Hogan, K., Von Moltke, L.L., Greenblatt, D.J., Court, M.H., 2004. Pharmacogenetic determinants of interindividual variability in bupropion hydroxylation by cytochrome P450 2B6 in human liver microsomes. Pharmacogenetics 14, 225–238. https://doi.org/10.1097/00008571-200404000-00002.

Hill, S.W., Varker, A.S., Karlage, K., Myrdal, P.B., 2009. Analysis of drug content and weight uniformity for half-tablets of 6 commonly split medications. J. Manag. Care Pharm. 15, 253–261. https://doi.org/10.18553/jmcp.2009.15.3.253.

IAPB Globally, 1.1 billion people were living with vision loss in 2020 Available online: https://www.iapb.org/learn/vision-atlas/magnitude-and-projections/global/.

Ju, H., McCloskey, B.D., Sagle, A.C., Kusuma, V.A., Freeman, B.D., 2009. Preparation and characterization of crosslinked poly(ethylene glycol) diacrylate hydrogels as fouling-resistant membrane coating materials. J. Memb. Sci. 330, 180–188. https://doi.org/10.1016/j.memsci.2008.12.054.

Kadry, H., Wadnap, S., Xu, C., Ahsan, F., 2019. Digital light processing (DLP)3D-printing technology and photoreactive polymers in fabrication of modified-release tablets. Eur. J. Pharm. Sci. 135, 60–67. https://doi.org/10.1016/j.ejps.2019.05.008.

Karakurt, I., Aydoğdu, A., Çıkrıkcı, S., Orozco, J., Lin, L., 2020. Stereolithography (SLA) 3D printing of ascorbic acid loaded hydrogels: A controlled release study. Int. J. Pharm. 584, 1–9. https://doi.org/10.1016/j.ijpharm.2020.119428.

Karalia, D., Siamidi, A., Karalis, V., Vlachou, M., 2021. 3d-printed oral dosage forms: mechanical properties, computational approaches and applications. Pharmaceutics 13. https://doi.org/10.3390/pharmaceutics13091401.

Karjiban, R.A., Basri, M., Rahman, M.B.A., Salleh, A.B., 2012. Structural properties of nonionic tween80 micelle in water elucidated by molecular dynamics simulation. APCBEE Proc. 3, 287–297. https://doi.org/10.1016/j.apcbee.2012.06.084.

Karoyo, A.H., Wilson, L.D., 2021. A review on the design and hydration properties of natural polymer-based hydrogels. Materials (basel). 14, 1–36. https://doi.org/10.3390/ma14051095.

Krkobabić, M., Medarević, D., Cvijić, S., Grujić, B., Ibrić, S., 2019. Hydrophilic excipients in digital light processing (DLP) printing of sustained release tablets: Impact on internal structure and drug dissolution rate. Int. J. Pharm. 572, 118790 https://doi.org/10.1016/j.ijpharm.2019.118790.

Madžarević, M., Ibrić, S., 2021. Evaluation of exposure time and visible light irradiation in LCD 3D printing of ibuprofen extended release tablets. Eur. J. Pharm. Sci. 158 https://doi.org/10.1016/j.ejps.2020.105688.

Martinez, P.R., Goyanes, A., Basit, A.W., Gaisford, S., 2018. Influence of geometry on the drug release profiles of stereolithographic (SLA) 3D-printed tablets. AAPS PharmSciTech 19, 3355–3361. https://doi.org/10.1208/s12249-018-1075-3.

Mazzoccoli, J.P., Feke, D.L., Baskaran, H., Pintauro, P.N., 2010. Mechanical and cell viability properties of crosslinked low and high MW PEGDA blends. J. Biomed. Mater. Res. A 93, 558–566. https://doi.org/10.1002/jbm.a.32563.Mechanical.

McCabe, D.J., McGillis, E., Willenbring, B.A., 2021. Clinical effects of intravenous bupropion misuse reported to a regional poison center. Am. J. Emerg. Med. 47, 86–89. https://doi.org/10.1016/j.ajem.2021.03.061.

McCann, R.M., Jackson, A.J., Stevenson, M., Dempster, M., McElnay, J.C., Cupples, M.E., 2012. Help needed inmedication self-management for people with visual impairment: Case-control study. Br. J. Gen. Pract. 62, 530–537. https://doi.org/10.3399/bjgp12X653570.

Melchels, F.P.W., Feijen, J., Grijpma, D.W., 2010. A review on stereolithography and its applications in biomedical engineering. Biomaterials 31, 6121–6130. https://doi.org/10.1016/j.biomaterials.2010.04.050.

Mini, E., Nobili, S., 2009. Pharmacogenetics: Implementing personalized medicine. Clin. Cases Miner. Bone Metab. 6, 17–24.

Nober, C., Manini, G., Carlier, E., Raquez, J.M., Benali, S., Dubois, P., Amighi, K., Goole, J., 2019. Feasibility study into the potential use of fused-deposition modeling to manufacture 3D-printed enteric capsules in compounding pharmacies. Int. J. Pharm. 569, 118581 https://doi.org/10.1016/j.ijpharm.2019.118581.

Overberg, A., Morton, S., Wagner, E., Froberg, B., 2019. Toxicity of bupropion overdose compared with selective serotonin reuptake inhibitors. Pediatrics 144. https://doi.org/10.1542/peds.2018-3295.

Pariskar, A., Sharma, P.K., Murty, U.S., Banerjee, S., 2023. Effect of tartrazine as photoabsorber for improved printing resolution of 3D printed “Ghost Tablets”: non-erodible inert matrices. J. Pharm. Sci. 112, 1020–1031. https://doi.org/10.1016/j.xphs.2022.11.014.

Patel, K., Allen, S., Haque, M.N., Angelescu, I., Baumeister, D., Tracy, D.K., 2015. Bupropion: a systematic review and meta-analysis of effectiveness as an antidepressant. Ther. Adv. Psychopharmacol. 6, 99–144. https://doi.org/10.1177/2045125316629071.

Peppas, P.L.R., N.A., 1987. A Simple equation for description of solute release I. Fickian and non-fickian release from non-swellable devices in the form of slabs, spheres, cylinders or discs. *J. Control. Release*, *5*, 23–36, doi:10.1016/S0168-3659(03)00195-0.

Peris, E., Bañuls, M.J., Maquieira, Á., Puchades, R., 2012. Photopolymerization as a promising method to sense biorecognition events. TrAC - Trends Anal. Chem. 41, 86–104. https://doi.org/10.1016/j.trac.2012.09.003.

Pezzullo, L., Streatfeild, J., Simkiss, P., Shickle, D., 2018. The economic impact of sight loss and blindness in the UK adult population. BMC Health Serv. Res. 18, 1–13. https://doi.org/10.1186/s12913-018-2836-0.

Protopapa, C., Siamidi, A., Kolipaka, S.S., Junqueira, L.A., Douroumis, D., Vlachou, M., 2024. In vitro profile of hydrocortisone release from three-dimensionally printed paediatric mini-tablets. Pharmaceutics 16, 385. https://doi.org/10.3390/pharmaceutics16030385.

Quan, H., Zhang, T., Xu, H., Luo, S., Nie, J., Zhu, X., 2020. Photo-curing 3D printing technique and its challenges. Bioact. Mater. 5, 110–115. https://doi.org/10.1016/j.bioactmat.2019.12.003.

Rekowska, N., Wulf, K., Koper, D., Senz, V., Seitz, H., Grabow, N., Teske, M., 2023. Influence of PEGDA molecular weight and concentration on the in vitro release of the model protein BSA–FITC from photo crosslinked systems. Pharmaceutics 15. https://doi.org/10.3390/pharmaceutics15041039.

Robles-Martinez, P., Xu, X., Trenfield, S.J., Awad, A., Goyanes, A., Telford, R., Basit, A.W., Gaisford, S., 2019. 3D printing of a multi-layered polypill containing six drugs using a novel stereolithographic method. Pharmaceutics 11. https://doi.org/10.3390/pharmaceutics11060274.

Rodríguez-Pombo, L., Xu, X., Seijo-Rabina, A., Ong, J.J., Alvarez-Lorenzo, C., Rial, C., Nieto, D., Gaisford, S., Basit, A.W., Goyanes, A., 2022. Volumetric 3D printing for rapid production of medicines. Addit. Manuf. 52, 102673 https://doi.org/10.1016/j.addma.2022.102673.

Rodríguez-Pombo, L., Martínez-Castro, L., Xu, X., Ong, J.J., Rial, C., García, D.N., González-Santos, A., Flores-González, J., Alvarez-Lorenzo, C., Basit, A.W., et al., 2023. Simultaneous fabrication of multiple tablets within seconds using tomographic volumetric 3D printing. Int. J. Pharm. X 5, 29–39. https://doi.org/10.1016/j.ijpx.2023.100166.

Saadabadi., M.R.H.A.S.A. Bupropion Available online: https://www.ncbi.nlm.nih.gov/books/NBK470212/.

Sheridan, D.C., Lin, A., Zane Horowitz, B., 2018. Suicidal bupropion ingestions in adolescents: increased morbidity compared with other antidepressants. Clin. Toxicol. 56, 360–364. https://doi.org/10.1080/15563650.2017.1377839.

Steinert, T., Fröscher, W., 2018. Epileptic seizures under antidepressive drug treatment: systematic review. Pharmacopsychiatry 51, 121–135. https://doi.org/10.1055/s-0043-117962.

Tagami, T., Nagata, N., Hayashi, N., Ogawa, E., Fukushige, K., Sakai, N., Ozeki, T., 2018. Defined drug release from 3D-printed composite tablets consisting of drug-loaded polyvinylalcohol and a water-soluble or water-insoluble polymer filler. Int. J. Pharm. 543, 361–367. https://doi.org/10.1016/j.ijpharm.2018.03.057.

Trenfield, Sarah J., Madla, Christine M., Basit, Abdul W., S.G. *The Shape of Things to Come: Emerging Applications of 3D* Printing *in Healthcare*; Springer, 2018; Vol. 31; ISBN 9783319907543.

Villanueva, E.L.D.; De Guzman Tarampi, J.; Cayetano, A.J.M.; Linsangan, N.B. Braille-based pillbox for visually impaired with audio reminder. In: *2020 4th Int. Conf. Electr. Telecommun. Comput. Eng. ELTICOM 2020 - Proc.* **2020**, 29–34, doi:10.1109/ELTICOM50775.2020.9230519.

Vithani, K., Maniruzzaman, M., Slipper, I.J., Mostafa, S., Miolane, C., Cuppok, Y., Marchaud, D., Douroumis, D., 2013. Sustained release solid lipid matrices processed by hot-melt extrusion (HME). Colloids Surfaces B Biointerfaces 110, 403–410. https://doi.org/10.1016/j.colsurfb.2013.03.060.

Vithani, K., Cuppok, Y., Mostafa, S., Slipper, I.J., Snowden, M.J., Douroumis, D., 2014. Diclofenac sodium sustained release hot melt extruded lipid matrices. Pharm. Dev. Technol. 19, 531–538. https://doi.org/10.3109/10837450.2013.805775.

Vlachou, M., Siamidi, A., Protopapa, C., Sotiropoulou, I., 2023. A review on the colours, flavours and shapes used in paediatric 3D printed oral solid dosage forms. RPS Pharm. Pharmacol. Reports 2, 1–11. https://doi.org/10.1093/rpsppr/rqad009.

Vlachou, M., Siamidi, A., 2023. Chrystalla Protopapa Extrusion-Based 3D Printing Methods for Oral Solid Dosage Forms. In: *3D & 4D Printing Methods for Pharmaceutical Manufacturing and Personalised Drug Delivery*. Springer, pp. 195–218.

Wang, J., Goyanes, A., Gaisford, S., Basit, A.W., 2016. Stereolithographic (SLA) 3D printing of oral modified-release dosage forms. Int. J. Pharm. 503, 207–212. https://doi.org/10.1016/j.ijpharm.2016.03.016.

Wasley, J., 2021. Identifying solutions to medication adherence in the visually impaired elderly. Build. Eng. 96, 32. https://doi.org/10.4140/tcp.n.2009.841.

Windham, B.G., Griswold, M.E., Fried, L.P., Rubin, G.S., Xue, Q.L., Carlson, M.C., 2005. Impaired vision and the ability to take medications. J. Am. Geriatr. Soc. 53, 1179–1190. https://doi.org/10.1111/j.1532-5415.2005.53376.x.